



## Chemical characteristics of North American surface layer outflow: Insights from Chebogue Point, Nova Scotia

Dylan B. Millet,<sup>1,2</sup> Allen H. Goldstein,<sup>1</sup> Rupert Holzinger,<sup>1,3</sup> Brent J. Williams,<sup>1</sup> James D. Allan,<sup>4</sup> José L. Jimenez,<sup>5</sup> Douglas R. Worsnop,<sup>6</sup> James M. Roberts,<sup>7</sup> Allen B. White,<sup>7</sup> Rynda C. Hudman,<sup>8</sup> Isaac T. Bertschi,<sup>9,10</sup> and Andreas Stohl<sup>11</sup>

Received 11 March 2006; revised 13 June 2006; accepted 3 July 2006; published 1 September 2006.

[1] We present a factor analysis-based method for differentiating air masses on the basis of source influence and apply the method to a broad suite of trace gas and aerosol measurements collected at Chebogue Point, Nova Scotia, during the summer of 2004 to characterize the chemical composition of atmospheric outflow from eastern North America. CO, ozone, and aerosol mass were elevated by 30%, 56%, and more than 300% at Chebogue Point during U.S. outflow periods. Organic aerosol mass was highest during U.S. pollution events, but made up the largest fraction (70%) of the total aerosol during periods of primary and especially secondary biogenic influence, indicating the importance of both anthropogenic and biogenic organic aerosol. Anthropogenic and oxygenated volatile organic compounds account for the bulk of the gas-phase organic carbon under most conditions; however, biogenic compounds are important in terms of chemical reactivity. Biogenic emissions thus have a significant impact on the chemistry of air masses downwind of the polluted northeastern United States. Using output from a global 3-D model of atmospheric composition (GEOS-Chem), we estimate that CO directly emitted from U.S. pollution sources makes up 28% of the total CO observed at Chebogue Point during U.S. outflow events and 19% at other times, although more work is needed to improve U.S. emission estimates for CO and other pollutants. We conclude that the effects of North American pollution on the chemistry of the western North Atlantic boundary layer are pervasive and not restricted to particular events.

**Citation:** Millet, D. B., et al. (2006), Chemical characteristics of North American surface layer outflow: Insights from Chebogue Point, Nova Scotia, *J. Geophys. Res.*, *111*, D23S53, doi:10.1029/2006JD007287.

### 1. Introduction and Background

[2] The urban-industrial northeastern United States is a major source of pollution to the global atmosphere, yet a quantitative understanding of how emissions from this region affect downwind atmospheric composition and

chemistry is lacking. The first step toward such an understanding is to characterize the chemical outflow. The International Consortium for Atmospheric Research on Transport and Transformation field experiment (ICARTT-2004) was carried out during the summer of 2004 specifically to address this issue (F. Fehsenfeld et al., International Consortium for Atmospheric Research on Transport and Transformation (ICARTT)–North America to Europe: Overview of the 2004 summer field study, submitted to *Journal of Geophysical Research*, 2006, hereinafter referred to as Fehsenfeld et al., submitted manuscript, 2006). Here we present an extensive suite of trace gas and aerosol measurements obtained at Chebogue Point, Nova Scotia, during the ICARTT-2004 campaign, develop a method for segregating air masses on the basis of the dominant source types, and apply the method to examine the chemistry and composition of boundary layer pollution outflow from the northeastern United States.

[3] Results from the 1993 North Atlantic Regional Experiment (NARE-1993) [Fehsenfeld et al., 1996] showed conclusively that North American emissions significantly alter atmospheric photochemistry over the North Atlantic and beyond. Summertime net ozone loss over the ocean, driven by peroxy radical chemistry at low NO<sub>x</sub>, is perturbed

<sup>1</sup>Division of Ecosystem Sciences, University of California, Berkeley, California, USA.

<sup>2</sup>Now at Department of Earth and Planetary Sciences, Harvard University, Cambridge, Massachusetts, USA.

<sup>3</sup>Now at Institute for Marine and Atmospheric Research, Utrecht University, Utrecht, Netherlands.

<sup>4</sup>School of Earth, Atmospheric and Environmental Science, University of Manchester, Manchester, UK.

<sup>5</sup>Department of Chemistry, University of Colorado, Boulder, Colorado, USA.

<sup>6</sup>Aerodyne Research Incorporated, Billerica, Massachusetts, USA.

<sup>7</sup>NOAA Earth System Research Laboratory, Boulder, Colorado, USA.

<sup>8</sup>Division of Engineering and Applied Sciences, Harvard University, Cambridge, Massachusetts, USA.

<sup>9</sup>Department of Interdisciplinary Arts and Sciences, University of Washington, Bothell, Washington, USA.

<sup>10</sup>Now at Hoefler Consulting Group, Inc., Anchorage, Alaska, USA.

<sup>11</sup>Norwegian Institute for Air Research, Kjeller, Norway.

by the presence of substantial layers of polluted air; such plumes have been sampled up to 1000 km from the coast [Daum *et al.*, 1996; Parrish *et al.*, 1998] and over Europe [Stohl and Trickl, 1999]. Ozone levels over the subtropical Atlantic are also affected by pollution from Africa and Europe [Lelieveld *et al.*, 2004].

[4] Anthropogenic emissions thus provide the main source of ozone over the temperate North Atlantic [Parrish *et al.*, 1993; Buhr *et al.*, 1996; Kasibhatla *et al.*, 1996]. Because of the export of NO<sub>x</sub> and peroxyacetyl nitrate (PAN), the total ozone pollution from U.S. emissions is about twice as large as that directly exported from the U.S. boundary layer [Liang *et al.*, 1998; Li *et al.*, 2004]. Modeling work by Kasibhatla *et al.* [1996] suggests that current ozone levels in the lower troposphere over the North Atlantic are at least twice as high as corresponding pre-industrial levels.

[5] Pollution export from North America is highly episodic [Atherton *et al.*, 1996; Berkowitz *et al.*, 1996; Knapp *et al.*, 1998; Parrish *et al.*, 1998; Li *et al.*, 2005], and characterized by vertical and horizontal heterogeneity [Angevine *et al.*, 1996b; Fast and Berkowitz, 1996; Moody *et al.*, 1996; Oltmans *et al.*, 1996; Wang *et al.*, 1996; Knapp *et al.*, 1998; Liang *et al.*, 1998]. During NARE-1993, surface sites such as Chebogue Point were frequently isolated from the overlying atmosphere by a low-level inversion [Angevine *et al.*, 1996a; Daum *et al.*, 1996; Kleinman *et al.*, 1996; Merrill and Moody, 1996; Parrish *et al.*, 1998]. It was concluded that pollutant transport primarily occurred aloft [Banic *et al.*, 1996; Fast and Berkowitz, 1996], with particular mixing conditions required to transport pollution to the surface layer and produce ozone episodes at Chebogue Point [Angevine *et al.*, 1996a]. Biogenic compounds interact with the anthropogenic pollutants and thus also play important roles in this region: formaldehyde at Chebogue Point during NARE-1993 was found to be 80% modern (i.e., nonfossil) carbon under all transport regimes suggesting a secondary biogenic source [Tanner *et al.*, 1996], and some model results indicate that isoprene nitrates make up a significant component of the NO<sub>x</sub> export flux [Horowitz *et al.*, 1998; Liang *et al.*, 1998].

[6] ICARTT-2004 consisted of multiple air, ship and ground based measurement platforms, deployed with the goal of observing the outflow of chemically and radiatively active gases and aerosols from North America, and developing constraints on sources, export, and chemical processing. Using in situ measurements to accomplish this requires a reliable way of determining air mass origin. Peak pollutant concentrations in North American outflow occur during flow transition periods [Draxler, 1996; Merrill and Moody, 1996], when back trajectory uncertainty is highest. In addition, while Chebogue Point is mostly isolated from local anthropogenic pollution, the separation of local from long-range signals presents significant problems in interpreting data from this and other sites. Coastal meteorology, and coupling between the marine boundary layer, planetary boundary layer, and free troposphere are difficult to represent accurately in chemical transport models. Other ways of differentiating air masses are therefore needed. Developing such a method and then applying it to characterize the

atmospheric chemistry of North American outflow are the objectives of this work.

[7] Here, we employ a factor analysis of the combined gas and aerosol data set to develop chemical fingerprints for the origins of sampled air masses, and use these fingerprints to examine the chemistry of North American outflow as a function of source influence. We also use output from the GEOS-Chem chemical transport model (CTM) to quantify the relative contributions of different source regions to observed CO concentrations, and to place the Chebogue Point findings in the larger context of North American outflow.

## 2. Methods

### 2.1. Field Site

[8] A ground-based field site was established as part of ICARTT-2004 at Chebogue Point (43.75°N, 66.12°W) during the summer of 2004 (1 July to 15 August), at the same site used during NARE-1993 (26 July to 3 September 1993). Sampling inlets were mounted on a 10 m scaffolding tower, and instruments were housed in climate-controlled laboratories at the tower base. Chebogue Point is located at the southwest tip of Nova Scotia, 9 km south-southwest of the town of Yarmouth. The Maine/New Brunswick coastline lies 130 km to the northwest across the Gulf of Maine. The cities of Boston and New York are 430 km and 730 km, respectively, to the southwest. Chebogue Point is in the Atlantic time zone (local standard time = UTC - 4). Further details of the site and its role in ICARTT-2004 are provided by Fehsenfeld *et al.* (submitted manuscript, 2006).

[9] Surface winds at the site were most frequently from the southeast to southwest (Figure 1). Northwesterly winds were also common, whereas winds out of the northeast (from Nova Scotia itself) were not. There was not a strong diel (24 hour) cycle in wind direction or speed, though there was a tendency for surface winds to back from southwesterly to west-southwesterly from 1200–1800 UTC (Figure 2), perhaps indicative of a weak sea breeze effect. While the most commonly occurring flow direction at the surface was from the southeast, radar wind profile measurements showed that winds above the marine boundary layer were predominantly southwesterly (Figure 2), with surface friction causing significant directional shear in the lowest few tens of meters. The nature of the air masses arriving at this site is affected strongly by both synoptic and complex local-scale meteorology, as described in detail by Merrill and Moody [1996] and Angevine *et al.* [1996a].

### 2.2. Measurements

[10] An extensive suite of volatile organic compounds (VOCs) was measured on site by two methods: in situ preconcentration followed by gas chromatography and mass selective/flame ionization detection (GC-MSD-FID), and proton-transfer reaction mass spectrometry (PTR-MS) [Lindinger *et al.*, 1998]. As described by Millet *et al.* [2005], the GC system was configured for analysis of C<sub>3</sub>–C<sub>6</sub> alkanes, alkenes, and alkynes on the FID channel, and a range of other VOCs, including aromatic, oxygenated, alkyl nitrate, and halogenated compounds on the MSD channel. For 30 min of each hour, two subsample flows (15 mL min<sup>-1</sup>) were drawn from the main sample line

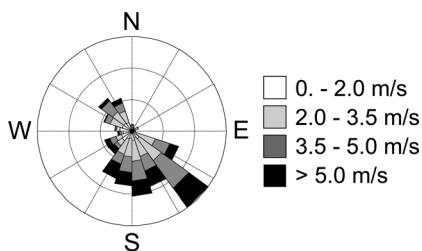


**Figure 1.** Wind rose plot for the ICARTT-2004 experiment. The lengths of the wedges are proportional to the frequency of observation.

( $4 \text{ L min}^{-1}$ ) and passed through a preconditioning trap for the removal of water ( $-25^\circ\text{C}$  cold trap). Carbon dioxide and ozone were scrubbed from the FID channel subsample (Ascarite II), and ozone was removed from the MSD channel subsample (KI impregnated glass wool). Preconcentration was accomplished using a combination of thermoelectric cooling ( $-15^\circ\text{C}$ ) and adsorbent trapping. Samples were injected into the GC by rapidly heating the trap assemblies to  $200^\circ\text{C}$ . The instrument was calibrated several times daily by dynamic dilution (factor of 1000) of ppm level standards (Scott Marin Inc. and Apel-Riemer Environmental Inc.) into zero air. Zero air was analyzed daily to check for blank problems and contamination for all measured compounds.

[11] As described in detail by R. Holzinger et al. (Emission, oxidation, and secondary organic aerosol formation of volatile organic compounds as observed at Chebogue Pt, Nova Scotia, submitted to *Journal of Geophysical Research*, 2006, hereinafter referred to as Holzinger et al., submitted manuscript, 2006), the PTR-MS was set up to monitor  $\sim 50$  individual masses in the selected ion mode during the first 30 min of every hour, and to do full mass scans (20–220 amu) during the second 30 min of every hour. A flow of  $500 \text{ mL min}^{-1}$  was maintained at all times resulting in a response time of 20 s. Background measurements were obtained by directing sample air through a catalytic converter (Pt-coated quartz wool heated to  $350^\circ\text{C}$ ). In the full mass scan mode ambient air was measured for 15 min followed by 15 min of background measurement, enabling detection of trace gases with an average concentration as low as 5 ppt. In the selected ion mode background and gas standards were measured 6 times a day (both for 15 min). Background concentrations were interpolated and subtracted from the ambient air signal on each monitored m/z ratio. Data presented here were collected in the selected ion mode; the sampling time matches that of the GC-MSD-FID system.

[12] PAN was measured by gas-chromatography and electron capture detection [Williams et al., 2000; Roberts et al., 2002]. The instrument used a continuously flushed sample loop which was injected every 5 min; the inlet equilibration time was estimated to be 1 min. The instrument response was calibrated every 10 hours using a modified acetone/NO photolysis source based on the calibrated NO mixing ratio and known conversion efficiency.

The detection limit and overall measurement uncertainty are estimated at 5 ppt and  $\pm(5 \text{ ppt} + 15\%)$ .

[13] Submicron aerosol mass and chemical composition were measured onsite at 1 min resolution by aerosol mass spectrometry [Jayne et al., 2000; Jimenez et al., 2003; J. D. Allan et al., Overview of in situ measurements of particle composition at Chebogue Point, Nova Scotia, during summer 2004 and insights into organic chemical processes, submitted to *Journal of Geophysical Research*, 2006, hereinafter referred to as Allan et al., submitted manuscript, 2006]. The AMS used thermal desorption ( $585^\circ\text{C}$ ), a quadrupole mass spectrometer and 70 eV electron impact ionization. The instrument measures mass concentrations for nonrefractory chemical species (e.g., nitrate, sulfate, organics and ammonium) in the 40–800 nm size range; transmission efficiency is reduced outside of this range. The methods used to process the AMS data are described by Allan et al. [2003, 2004]. The AMS data were validated by comparing with 24 hour integrated aerosol samples analyzed by ion chromatography, and with aerosol volume distributions measured using a differential mobility particle sizer. For more details see Allan et al. (submitted manuscript, 2006). For this analysis we use 30 min averages of the AMS data which coincide with the GC-MSD-FID sampling times.

[14] Submicron black carbon was measured using a multiangle absorption photometer (MAAP; Thermo Environmental Inc., model 5012), assuming a specific absorbance of  $1.5 \times 10^5 \mu\text{g m}^{-2}$ . Radon ( $^{222}\text{Rn}$ ) gas was measured with a dual-flow loop, two-filter radon detector (ANSTO Inc.).  $\text{CO}_2$  and CO were measured by nondispersive infrared (NDIR) absorption (LiCor Inc., model 6262) and gas filter correlation, NDIR absorption (Thermo Environmental Inc., model 48C), respectively. Ozone was measured using a UV photometric  $\text{O}_3$  analyzer (Dasibi Inc., model 1008-RS). Incoming photosynthetically active radiation was measured with a quantum sensor (LiCor Inc.,

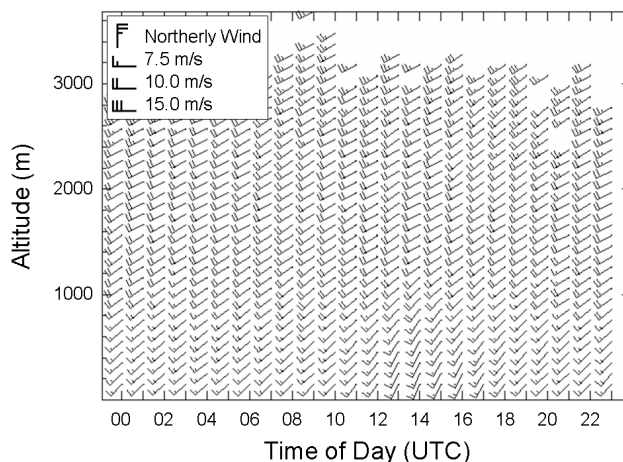


**Figure 2.** Mean diel cycle in wind direction and speed at Chebogue Point during ICARTT-2004, as measured by the radar wind profiler (White et al., submitted manuscript, 2006a). Above the marine boundary layer, the winds are predominantly from the southwest.

model 190SZ). Wind speed and direction were monitored with a propeller wind monitor (R.M. Young Co.) mounted on a 3 m tower on top of the laboratory container, and ambient air temperature was measured using a temperature and relative humidity probe (Vaisala Inc., model HMP45C). Height-resolved three-dimensional wind profiles above Chebogue Point were obtained using a radar wind profiler [Carter *et al.*, 1995; A. B. White *et al.*, A wind profiler trajectory tool for air quality transport applications, submitted to *Journal of Geophysical Research*, 2006a, hereinafter referred to as White *et al.*, submitted manuscript, 2006a; A. B. White *et al.*, Comparing meteorological controls on air quality during the NEAQS (2002) and ICARTT (2004) field campaigns, submitted to *Journal of Geophysical Research*, 2006b]. For this analysis we averaged the higher-resolution data to match the 1-hour VOC time base.

[15] Additional measurements made at the site (not reported here) include online organic aerosol composition by thermal desorption GC-MSD [Williams *et al.*, 2006; B. J. Williams *et al.*, Chemical speciation of organic aerosol during ICARTT 2004: Results from in situ measurements, submitted to *Journal of Geophysical Research*, 2006, hereinafter referred to as Williams *et al.*, submitted manuscript, 2006], aerosol organic functional group composition every 5–24 hours using Fourier transform infrared spectrometry [Maria and Russell, 2005], speciated  $\text{NO}_y$  by thermal dissociation and laser induced fluorescence [Day *et al.*, 2002], particle number density and size distribution [Allan *et al.*, submitted manuscript, 2006], total gaseous mercury using a mercury vapor analyzer (Tekran Instruments Inc., model 2537A) [Kellerhals *et al.*, 2003], aerosol scattering, absorption, and optical depth [Sheridan *et al.*, 2001; Delene and Ogren, 2002], aerosol elemental composition every 3 hours using eight-stage rotating drum impactors and synchrotron x-ray fluorescence [VanCuren *et al.*, 2005], size resolved aerosol total mass and inorganic chemistry [Quinn *et al.*, 2000],  $\text{SO}_2$  (Thermo Electron Inc., model 43S), vertical profiles of aerosol structure and optical properties obtained with a Raman lidar using a Nd:YAG laser transmitting at 532 nm (T. J. Duck *et al.*, Transport of forest fire emissions from Alaska and the Yukon Territory to Nova Scotia during summer 2004, submitted to *Journal of Geophysical Research*, 2006, hereinafter referred to as Duck *et al.*, submitted manuscript, 2006), as well as ozone sonde releases from Yarmouth. For more details on the analytical methods used at Chebogue Point, including instrument performance, we refer the reader to the references cited above and to Fehsenfeld *et al.* (submitted manuscript, 2006).

### 2.3. Model Description

[16] The atmospheric distribution of CO was simulated for the ICARTT-2004 period using the GEOS-Chem global 3D CTM [Bey *et al.*, 2001; Park *et al.*, 2004]. GEOS-Chem (version 7.02, <http://www-as.harvard.edu/chemistry/trop/geos/index.html>) uses GEOS-4 assimilated meteorological data from the NASA Goddard Earth Observing System, including winds, convective mass fluxes, mixing depths, temperature, precipitation, and surface properties. The data have 6-hour temporal resolution (3-hour for surface variables and mixing depths),  $1^\circ \times 1.25^\circ$  horizontal resolution, and 55 vertical layers. We degrade the horizontal resolution to  $2^\circ \times 2.5^\circ$  for input to GEOS-Chem.

[17] Global emissions are as described by Bey *et al.* [2001], with recent updates [Martin *et al.*, 2002; Park *et al.*, 2004; Xiao *et al.*, 2004]. Anthropogenic emissions from North America are based on the EPA NEI 1999 v.1 inventory (NEI99, <http://www.epa.gov/ttn/chief/net/1999inventory.html>), with modifications (R. C. Hudman *et al.*, Surface and lightning sources of nitrogen oxides over the United States: Magnitudes, chemical evolution, and outflow, submitted to *Journal of Geophysical Research*, 2006, submitted manuscript, 2006, hereinafter referred to as Hudman *et al.*, manuscript in preparation, 2006; R. C. Hudman *et al.*, Characterization of the North American ozone-CO correlations during the ICARTT study, manuscript in preparation, 2006, hereinafter referred to as Hudman *et al.*, manuscript in preparation, 2006). In particular, on-road CO transport emissions have been reduced by 50% to correct a corresponding factor of two overestimate in the NEI99 inventory [Parrish, 2006; Hudman *et al.*, manuscript in preparation, 2006]. This results in a 30% reduction of the total anthropogenic CO source from North America (from 7.3 to 5.1 Tg CO per month for July and August).

[18] Individual sources are tagged in order to resolve the origin of CO at Chebogue Point. We use separate tracers to track CO from U.S. fossil fuel, U.S. biomass burning, Canada (+Alaska) fossil fuel, Canada (+Alaska) biomass burning, Asia, Europe, chemical production from methane and VOCs, and other sources. OH fields are taken from archived monthly mean 3-D fields of tropospheric OH concentrations from a GEOS-Chem full-chemistry simulation. The current simulation was conducted at  $2^\circ \times 2.5^\circ$  horizontal resolution and with 30 vertical layers. Results are presented here for July and August 2004, and follow a 1 year spin-up. Applications of GEOS-Chem to simulation of other aspects of ICARTT-2004 data include analyses of North American  $\text{NO}_x$  emissions and reactive nitrogen export (Hudman *et al.*, submitted manuscript, 2006), ozone production efficiency and export (Hudman *et al.*, manuscript in preparation, 2006), boreal fire emissions (S. Turquety *et al.*, Inventory of boreal fire emissions for North America in 2004: The importance of peat burning and pyro-convective injection, submitted to *Journal of Geophysical Research*, 2006, hereinafter referred to as Turquety *et al.*, submitted manuscript, 2006), and Asian inflow (Q. Liang *et al.*, Summertime influence of Asian pollution in the free troposphere over North America, submitted to *Journal of Geophysical Research*, 2006, hereinafter referred to as Liang *et al.*, submitted manuscript, 2006).

### 2.4. Factor Analysis

[19] Here we develop a method to separate and characterize the dominant sources of trace gases and aerosols impacting air arriving at Chebogue Point during the summer of 2004. The approach is based on a factor analysis [e.g., Lamanna and Goldstein, 1999; Wang *et al.*, 2003; Millet *et al.*, 2004; Kim *et al.*, 2005] of the in situ data set using principal factors extraction with varimax rotation. Factor analysis identifies correlations among variables that are driven by common processes such as sources, transport, and chemistry. Here we focus on a suite of VOCs and related trace gas and aerosol tracers that were measured at hourly or greater frequency and which have at least 80% data coverage (Table 1). Application of factor analysis to

**Table 1.** Tracers Used for Factor Analysis

Species	Valid Hourly Data Points	Concentration	
		Median	IQR <sup>a</sup>
Propane, ppt	886	215	126–321
Isobutane, ppt	886	27	15–48
Butane, ppt	886	36	19–60
Isopentane, ppt	886	30	17–59
Hexane, ppt	886	8	5–12
Propene, ppt	886	13	10–18
1-butene, ppt	886	3	2–4
Pentane, ppt	886	21	13–32
t-2-pentene, ppt	886	3	2–4
1-pentene, ppt	886	2	2–3
2- and 3-methylpentane, ppt	886	11	6–19
Heptane, ppt	864	5	3–6
Benzene, ppt	887	32	21–44
C <sub>2</sub> Cl <sub>4</sub> , ppt	886	6	5–8
Toluene, ppt	887	15	7–31
CH <sub>3</sub> Cl, ppt	869	600	550–657
Isoprene, ppt	887	10	5–29
MTBE, ppt	886	10	6–17
HCFC-141b, ppt	887	17	16–18
Acetaldehyde, ppt	887	179	120–253
Dimethylsulfide, ppt	887	91	53–143
Propanal, ppt	887	35	26–47
Methyl iodide, ppt	887	10	8–12
2-methyl-propanal, ppt	887	10	7–13
Acetone, ppt	887	884	593–1178
Butanal, ppt	887	26	21–32
Methacrolein, ppt	887	20	13–29
Methanol, ppt	887	1389	865–2078
Methyl ethyl ketone, ppt	887	44	29–67
Methylene chloride, ppt	875	34	30–39
Methyl nitrate, ppt	887	4	3–4
Isopropanol, ppt	884	11	7–16
Ethanol, ppt	887	107	63–190
Methyl vinyl ketone, ppt	887	16	10–31
Ethyl nitrate, ppt	886	4	3–5
Isopropyl nitrate, ppt	887	6	4–8
2-pentanone, ppt	867	5	3–7
3-pentanone, ppt	867	5	3–8
Acetonitrile, ppt	887	57	47–70
Alpha-pinene, ppt	887	6	4–17
n-propyl nitrate, ppt	886	3	2–4
2-butyl nitrate, ppt	887	4	2–6
Beta-pinene, ppt	875	3	0–13
Ethylbenzene, ppt	887	2	1–4
p-xylene, ppt	887	2	1–3
m-xylene, ppt	887	3	2–6
Carene, ppt	887	1	0–4
o-xylene, ppt	850	2	1–4
CO, ppb	853	128	111–143
Ozone, ppb	871	31	23–41
CO <sub>2</sub> , ppm	851	373	369–378
Radon-222, mBq m <sup>-3</sup>	855	1470	665–2075
Aerosol sulfate, μg m <sup>-3</sup>	725	0.58	0.25–1.29
Aerosol organic matter, μg m <sup>-3</sup>	725	1.52	0.63–3.2
Aerosol ammonium, μg m <sup>-3</sup>	725	0.22	0.11–0.44
Aerosol nitrate, μg m <sup>-3</sup>	725	0.09	0.05–0.21
PAN, ppt	804	64	26–125

<sup>a</sup>IQR, interquartile range.

other aspects of ICARTT-2004 include analyses of organic aerosol speciation (Williams et al., submitted manuscript, 2006), biogenic VOC chemistry (Holzinger et al., submitted manuscript, 2006), Asian inflow (Liang et al., submitted manuscript, 2006), and aerosol optical properties (P. Quinn et al., Impacts of sources and aging on aerosol properties in the marine boundary layer across the Gulf of Maine, submitted to *Journal of Geophysical Research*, 2006).

[20] Six factors were extracted from the combined trace gas and aerosol data set, accounting for 60% of the total variance. Including another factor failed to explain more than an additional 2% of the cumulative variance. The degree of association between a factor and a given chemical species is given by a loading value, with the maximum loading equal to one. Compound loadings (above a thresh-

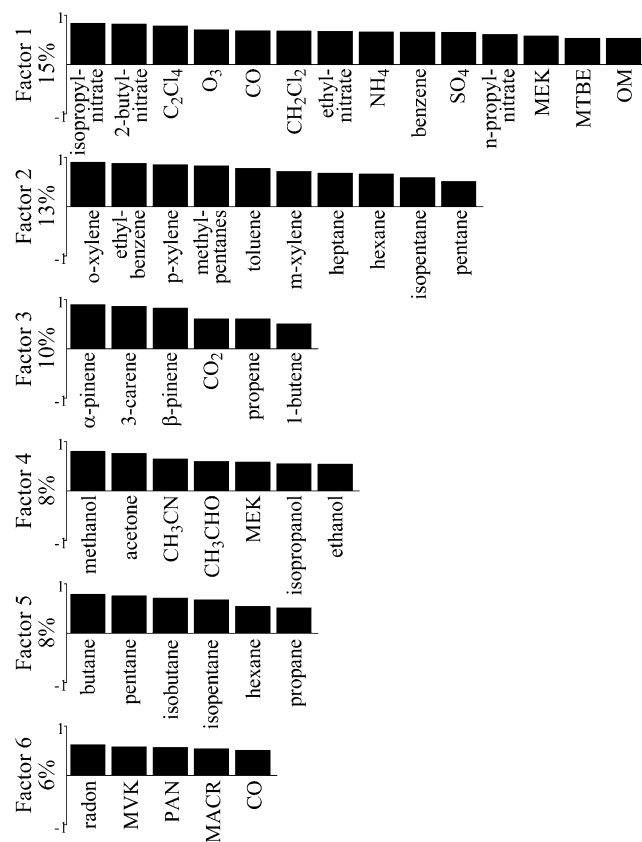


**Figure 3.** Factor analysis results. Loadings  $< 0.5$  are omitted. MEK, methyl ethyl ketone; MTBE, methyl t-butyl ether; OM, particulate organic matter; MVK, methyl vinyl ketone; PAN, peroxyacetyl nitrate; MACR, methacrolein.

old of 0.5) and the wind direction dependence for each factor are displayed in Figures 3 and 4.

[21] Factor 1 accounts for 15% of the cumulative variance and consists of urban and industrial pollutants as well as the photochemical products of such emissions. All of the associated species have atmospheric lifetimes longer than a few days, and local wind observations and wind profiler back trajectories (White et al., submitted manuscript, 2006a) show the southerly origin of this factor (Figures 4 and 5), which clearly reflects outflow from the northeastern United States. Note that while the industrialized U.S. coast lies to the southwest of the site, the surface winds were frequently from the south or south-southeast during factor 1 episodes. However, the prevailing winds above the marine boundary layer were from the southwest (Figure 2), with directional shear near the surface due to friction. Thus if shear-induced turbulent mixing has occurred along the trajectory, U.S. pollution may be observed at the surface despite southeasterly winds. As a result, the surface winds are not sufficient to monitor the transport direction. This underscores the value of including in situ chemical measurements in trajectory analyses, especially for sites with complex meteorology such as Chebogue Point. Factor 1 enhancements occurred at all times of day, but were most frequent from 1200 to 1800 local time (1600 to 2200 UTC). The strong association of the alkyl nitrates with factor 1 is consistent with the findings

of Roberts et al. [1996], who showed that such compounds are good indicators of photochemical pollution at Chebogue Point. Below we use this factor as a fingerprint of U.S. pollution.

[22] The second factor, which accounts for 13% of the cumulative variance, is composed of combustion tracers that are shorter-lived than those associated with factor 1, with lifetimes ranging from a few hours to 1.5 days at  $[OH] = 2 \times 10^6$  molecules  $\text{cm}^{-3}$  (the diel average OH concentration below 800 hPa at Chebogue Point as simulated with the GEOS-Chem model). While the back trajectories do not resolve a clear region of origin, local wind observations show it to be distinct from that of factor 1 (Figure 4). Factor 2 was enhanced during occasional brief episodes, most frequently with winds from the northwest and the town of Yarmouth during the night and early morning, and we attribute this factor to local anthropogenic emissions from Yarmouth and adjacent areas. These local plumes had undergone only limited photochemical processing: they did not contain the high levels of secondary pollutants, such as alkyl nitrates and ozone, seen with the more processed plumes from the northeastern United States.

[23] The monoterpenes and carbon dioxide load with the third factor, which we attribute to local biogenic emissions, and which accounts for 10% of the cumulative variance. Propene and 1-butene, also known to be emitted by terrestrial plants [Goldstein et al., 1996], are associated with this factor as well. Enhancements typically occurred during the night and early morning, when the terrestrial biosphere is a net source of respired  $\text{CO}_2$  and vertical mixing is limited. Monoterpene emissions are temperature-dependent and highest during the day; however, concentrations are frequently highest at night when photochemical loss and dilution are diminished [Lamanna and Goldstein, 1999]. The local wind direction (Figure 4) show that these biogenic emissions originate mainly from the forests of Nova Scotia to the north and northeast. There may also be a contribution from local pasture emissions under very stable or light wind conditions.

[24] The fourth factor, accounting for 8% of the cumulative variance, consists of oxygenated VOCs (OVOCs), along with acetonitrile, which is thought to be emitted almost exclusively from biomass burning [Lobert et al., 1990; Li et al., 2003]. The associated OVOCs are also emitted from fires [Yokelson et al., 1996; Holzinger et al., 1999; Andreae and Merlet, 2001], and produced in the atmosphere during the photochemical processing of the fire plume [Goode et al., 2000; Jost et al., 2003; Yokelson et al., 2003; Holzinger et al., 2005; Trentmann et al., 2005]. However, OVOCs also have a number of other important sources, in particular the terrestrial biosphere [Schade and Goldstein, 2001; Jacob et al., 2002; Karl et al., 2003; Jacob et al., 2005], as well as urban emissions [Goldan et al., 1995; Grosjean et al., 2001; de Gouw et al., 2005]. Back trajectories (not shown) and local wind direction do not indicate a clear source region for factor 4, which likely represents biomass burning emissions or cotransport of pyrogenic and biogenic emissions. There were extensive boreal fires in Alaska and northern Canada during the ICARTT-2004 study period, the effects of which were widespread [Pfister et al., 2005; de Gouw et al., 2006; Duck et al., submitted manuscript, 2006; Turquetly et al.,

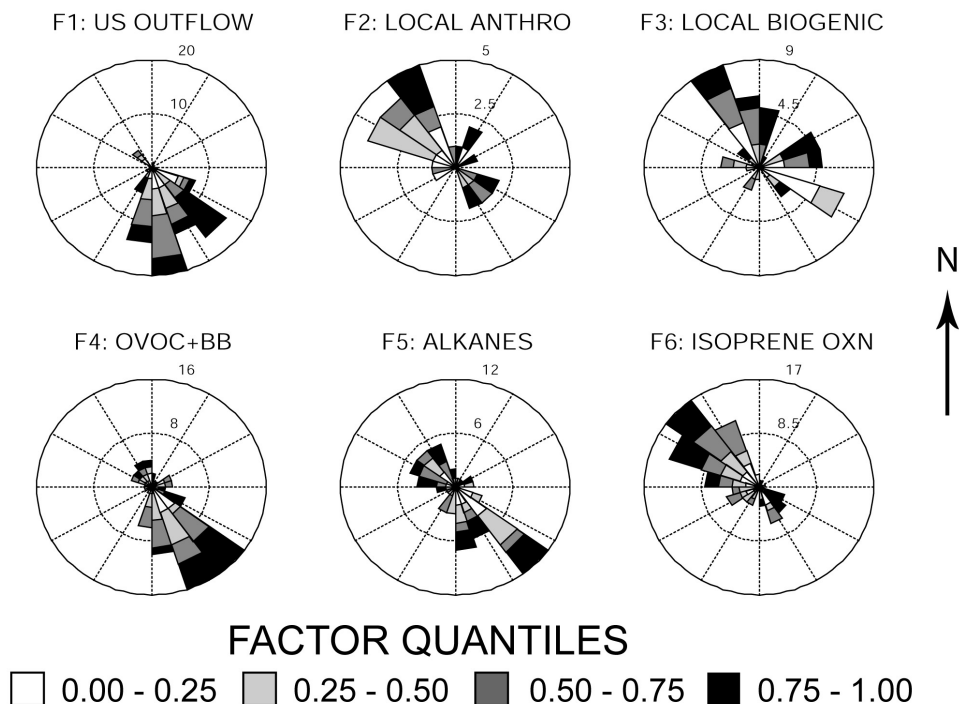


**Figure 4.** Wind direction dependence for the six chemical factors at Chebogue Point. The wedges are color coded according to the quartiles for each factor, and their length is proportional to the frequency of observation.

submitted manuscript, 2006; M. Val Martin, Significant enhancements of nitrogen oxides, black carbon and ozone in the North Atlantic lower free troposphere resulting from North American boreal wildfires, submitted to *Journal of Geophysical Research*, 2006]. Since any effect from these fires on sampled air masses would have occurred more than 48 hours upwind, their influence cannot be resolved solely from back trajectories. Enhancements in factor 4 occurred at all times of day, but were most common in the afternoon (1200–1800 local time).

[25] The alkanes group together on factor 5, which accounts for 8% of the cumulative variance. The back trajectories and local wind direction do not indicate a clear source region (as with factor 2), and factor 5 did not exhibit a significant diel cycle. Factor 5 may result from local and regional emissions of light alkanes from liquefied petroleum gas (LPG) use and handling. Specific nearby sources include an LPG storage facility and harbor facilities in Yarmouth. Removal processes and dynamics can also lead to factors, however, and factor 5 could reflect the same source as factor 2: a generalized, local anthropogenic source which is separated into two factors according to the degree of aging, with the shorter-lived species on one factor and the longer-lived ones on the other.

[26] Factor 6 accounts for 6% of the cumulative variance, and is defined by enhanced levels of the isoprene oxidation products methyl vinyl ketone (MVK) and methacrolein (MACR), in addition to  $\text{Rn}^{222}$ , PAN, and CO. We conclude that this factor represents photochemically processed biogenic emissions, in particular isoprene. Its influence was highest with winds from the northwest and mainland Canada, and during the middle of the day.  $\text{Rn}^{222}$ , which is

emitted from soils and undergoes radioactive decay with a half-life of  $\sim 4$  days, reflects the terrestrial origins of factor 6. Since the atmospheric lifetime of  $\text{Rn}^{222}$  exceeds that of isoprene and its oxidation products (1–7 hours at  $[\text{OH}] = 2 \times 10^6 \text{ molecules cm}^{-3}$ ), air masses with elevated MVK

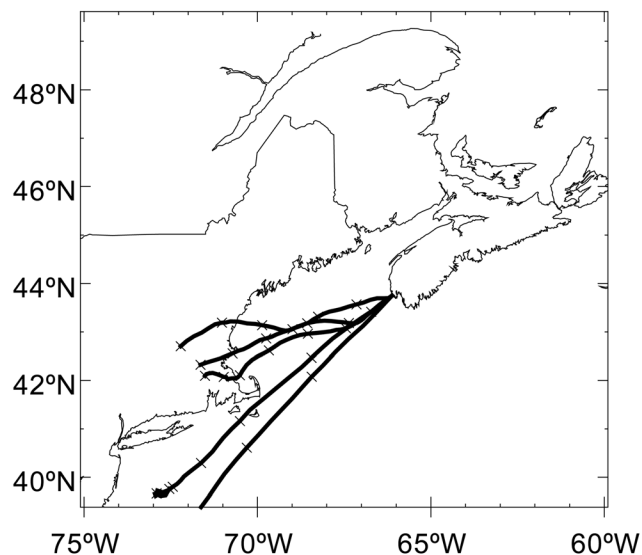


**Figure 5.** Thirty-six-hour wind profiler back trajectories (White et al., submitted manuscript, 2006a) for U.S. outflow events. Trajectories shown reflect the highest-scoring episodes for factor 1 which are separated by  $>1$  day. Crosses indicate 6 hour time intervals along the back trajectories.

and MACR also contain elevated  $Rn^{222}$ . There is also a weak  $Rn^{222}$  influence on factor 1 (loading = 0.4), but not on factors 2–5, indicating less mixing in the continental boundary layer during the days prior to arrival at Chebogue Point. PAN, which loads most strongly on factor 6 (loading = 0.6), but also on factor 1 (loading = 0.4), is produced during the photochemical processing of isoprene and other biogenic and anthropogenic VOCs. As a result, we see elevated PAN both with aged anthropogenic (factor 1) and biogenic (factor 6) emissions, but not with the other, less processed local factors. The association of both PAN and CO with factor 6 may also reflect transport of higher background mixing ratios from more northerly latitudes. The importance of this biogenic VOC oxidation factor for regional atmospheric chemistry and particle formation is examined in detail by Holzinger et al. (submitted manuscript, 2006).

[27] Aerosol organic matter (OM) loaded most strongly on factor 1 (loading = 0.5), indicating U.S. pollution as the dominant source of elevated aerosol OM in this region. However, OM also loaded on the biogenic factor 6 (isoprene oxidation; loading = 0.3) and on factor 4 (OVOC + biomass burning; loading = 0.4), so other, nonurban sources are also important for the OM budget. This issue is examined in more detail in section 3.2, and by several other papers in this special issue of JGR (Allan et al., submitted manuscript, 2006; Holzinger et al., submitted manuscript, 2006; Williams et al., submitted manuscript, 2006).

[28] Both dimethyl sulfide (DMS) and methyl iodide were included in the factor analysis, but they did not load strongly with any of the other compounds. DMS only had a weak correlation with factor 3 (local biogenic; loading = 0.3), which we take to represent a common dependence on meteorology: elevated concentrations when vertical mixing is limited. The lack of a strong relationship between the six factors and these two oceanic tracers indicates that if air-sea exchange is a major source of variability for other measured compounds, then the spatial or temporal signatures differ from those of DMS and methyl iodide.

[29] While the amount of variance explained does not necessarily imply the importance of a source type or factor for atmospheric chemistry, the time periods impacted by a particular source can be identified with factor analysis, and then used to investigate the chemical characteristics and importance of that source for atmospheric composition.

### 3. Air Mass Segregation Based on Chemical Factors

[30] We use the six factors described above to differentiate air masses on the basis of source influence. The factor scores, which are linear combinations of the input variables, are scaled to have a mean of zero and a standard deviation of one. We define “impact periods” for each factor as those times when the factor score is  $>1$  (i.e., its contribution is one standard deviation above the mean). This criterion does not imply that a given source is the sole contributor to atmospheric composition; rather it identifies periods when that source was an important ( $>1\sigma$ ) influence on air arriving at Chebogue Point. This allows for the isolation of time periods based on distinct types of events impacting atmospheric composition at the site.

[31] Timelines for the six factors are shown in Figure 6. According to our  $1\sigma$  criterion, U.S. outflow significantly impacted atmospheric composition at Chebogue Point 15% of the time. The mean duration of such episodes was 7.0 hours. By contrast, local anthropogenic emissions were important only 5% of the time, and the mean episode length was short (1.6 hours). The difference in episode duration is consistent with what we would expect for distant versus local sources. The local biogenic, OVOC + biomass burning, and alkane factors all had impact frequencies of 9–15%, with associated timescales ranging from 3 to 4 hours. The isoprene oxidation factor was important 16% of the time, with a mean episode length of 4.9 hours. Impact periods for the six factors collectively account for 50% of the observations; the remaining data reflect both clean marine air and air influenced by the identified source types (but at  $<1\sigma$ ). Below, we examine the effect these event types have on CO, ozone, aerosol mass, and the budget of organic gases and aerosols.

#### 3.1. CO and Ozone

[32] CO and ozone mainly loaded on factor 1, indicating that U.S. outflow is the main source of variability for these compounds. The overall distributions of ozone and CO in air arriving at Chebogue Point in 2004 were very similar to 1993, though NARE-1993 featured one pollution episode outside the range of what was observed in 2004. Ozone mixing ratios measured at Chebogue Point averaged 33 ppb (0.05–0.95 quantiles: 15–57 ppb) during ICARTT-2004, and 34 (16–59) ppb in 1993. CO averaged 126 ppb in both years, with a slightly wider distribution in 2004 (0.05–0.95 quantiles: 93–176 in 1993 and 77–171 in 2004).

[33] Applying our criterion for U.S. pollution (factor 1  $>1$ ), we can quantify how much CO and ozone were elevated during periods of U.S. outflow. During factor 1 episodes, ozone concentrations increased by 56% to  $50 \pm 7$  ppb (mean  $\pm 1\sigma$ ), compared to  $32 \pm 12$  ppb at all other times. CO mixing ratios increased by 30% to  $160 \pm 19$  ppb, compared to  $123 \pm 26$  ppb during other periods. Age spectra computed with the FLEXPART model [Stohl et al., 1998; Stohl and Thomson, 1999] indicate that the excess CO observed during these U.S. pollution periods was predominantly emitted between 2 and 3 days prior to arrival at Chebogue Point (Figure 7). While the age spectra of Figure 7 suggest that CO should be elevated by  $\sim 90$  ppb during outflow periods, the measurements show an increase of only 37 ppb. This discrepancy points to a significant overestimate of U.S. CO emissions in the NEI99 inventory, as concluded by other recent studies [Parrish, 2006; Hudman et al., manuscript in preparation, 2006].

#### 3.2. Aerosol Mass and Composition

[34] Both the total aerosol mass and its chemical makeup were strongly dependent on the event types identified using the factor analysis. Overall, the submicron aerosol mass ranged from  $0.3 \mu\text{g m}^{-3}$  (0.05 quantile) to  $17 \mu\text{g m}^{-3}$  (0.95 quantile), with a mean of  $4 \mu\text{g m}^{-3}$ . Aerosol mass loading was higher by more than a factor of 3 during U.S. pollution outflow periods, increasing to an average of  $13 \pm 8 \mu\text{g m}^{-3}$ . The aerosol mass was also elevated during OVOC + biomass burning impact periods, probably reflecting the

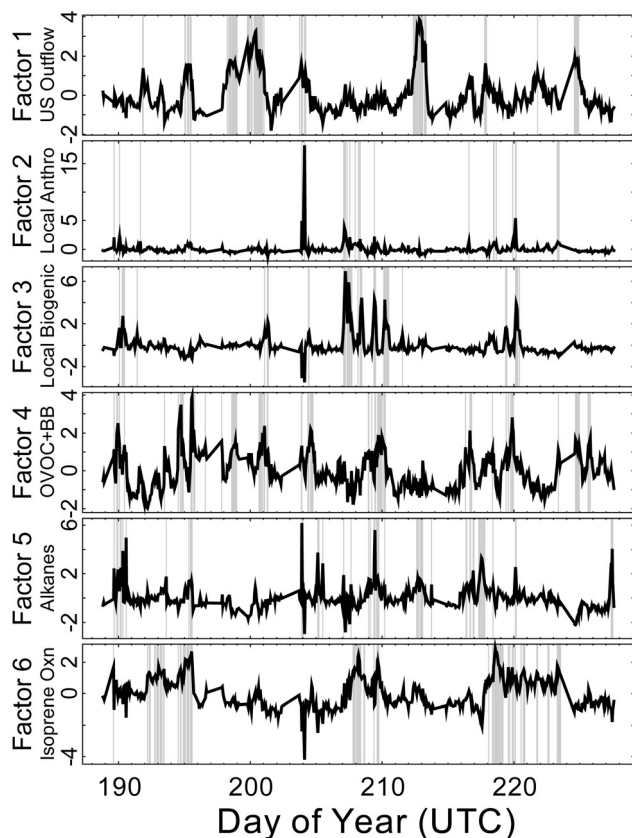


**Figure 6.** Timelines for the six chemical factors. Shaded regions represent impact periods (factor score  $> 1\sigma$ ) for each.

analogous range of sources for OVOCs and aerosols (combustion, biogenic emissions, and secondary production).

[35] Organic matter is a major component of the atmospheric aerosol, and current understanding of organic aerosol composition and formation mechanisms is clearly inadequate [Heald *et al.*, 2005]. At Chebogue Point, the amount of organic aerosol correlated most strongly with U.S. pollution (loading = 0.5), which is in agreement with the findings of *de Gouw et al.* [2005]. It also loaded moderately on factor 4 (OVOC + biomass burning, loading = 0.4) and factor 6 (isoprene oxidation, loading = 0.3). However, organic matter made up the largest fraction of the total aerosol mass during periods of secondary biogenic influence: 74%, compared to 36% during U.S. outflow events (Figure 8 and Table 2). In addition to making up a large fraction of the aerosol mass during these times, biogenic secondary organic aerosol (SOA) was also important in an absolute sense. OM during factor 6 (isoprene oxidation) periods averaged  $3.53 \mu\text{g m}^{-3}$ , compared to  $2.08 \mu\text{g m}^{-3}$  during all other times (i.e., including all other types of events, including U.S. pollution), and  $1.41 \mu\text{g m}^{-3}$  during nonevent periods (Table 2). This indicates that biogenic SOA makes a significant contribution to aerosol OM at this site, both in a relative sense and in terms of absolute mass, as is discussed in more detail by Allan *et al.* (submitted manuscript, 2006), Holzinger *et al.* (sub-

mitted manuscript, 2006), and Williams *et al.* (submitted manuscript, 2006).

### 3.3. Gas-Phase Organic Carbon Budget and Reactivity

[36] Here we examine the budget and chemical reactivity of gas phase organic carbon in the form of VOCs, and their dependence on the source factors. The total VOC abundance, expressed in ppb of carbon (ppbC), represents the total amount of nonmethane organic carbon that can ultimately react to form ozone or SOA. The median measured VOC abundance measured at Chebogue Point during ICARTT-2004 was 12 ppbC, which agrees well with the median value of 11 ppbC observed during NARE-1993 [Roberts *et al.*, 1998] (both values exclude the  $\text{C}_2$  hydrocarbons).

[37] In contrast to CO, ozone, and particulate matter, VOC abundance was only marginally higher during periods of U.S. outflow compared to all other times, increasing from  $15 \pm 6$  to  $17 \pm 4$  ppbC. The distribution during factor 1 episodes is slightly narrower, since the other time periods include both extremely clean oceanic air masses and those containing local and regional emissions. Anthropogenic emissions constitute 25–40% of the gas-phase organic carbon under all flow regimes (Figure 8 and Table 2). OVOCs are also very important at all times. Except during periods of local influence (factors 3 and 6), primary biogenic compounds generally make up a nonnegligible but relatively minor portion of the gas-phase organic carbon at Chebogue Point.

[38] This picture changes substantially, however, if we take into account the chemical reactivity of the different gases. Here we use the product of VOC number density with the rate constant for chemical loss by OH (the VOC OH reactivity,  $\text{s}^{-1}$ ) to identify the VOCs that are driving atmospheric photochemistry. The VOC OH reactivity represents the loss rate for OH due to the various VOCs. Figure 8 displays this quantity for different groups of compounds.

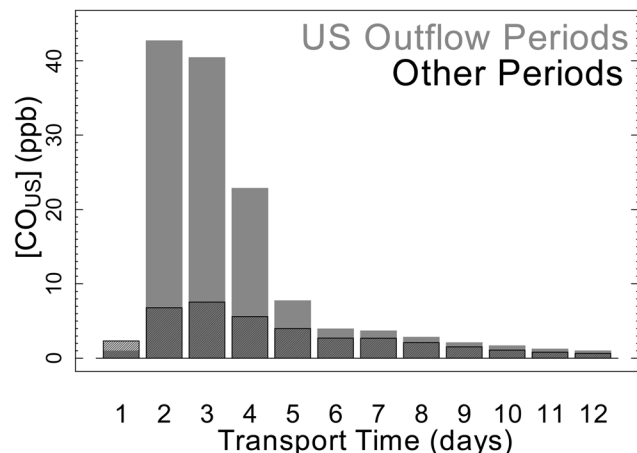


**Figure 7.** Age spectra for U.S. pollution CO arriving at Chebogue Point, calculated using the FLEXPART model [Stohl *et al.*, 1998; Stohl and Thomson, 1999]. During U.S. outflow events, the excess CO was predominantly emitted 2–3 days prior.

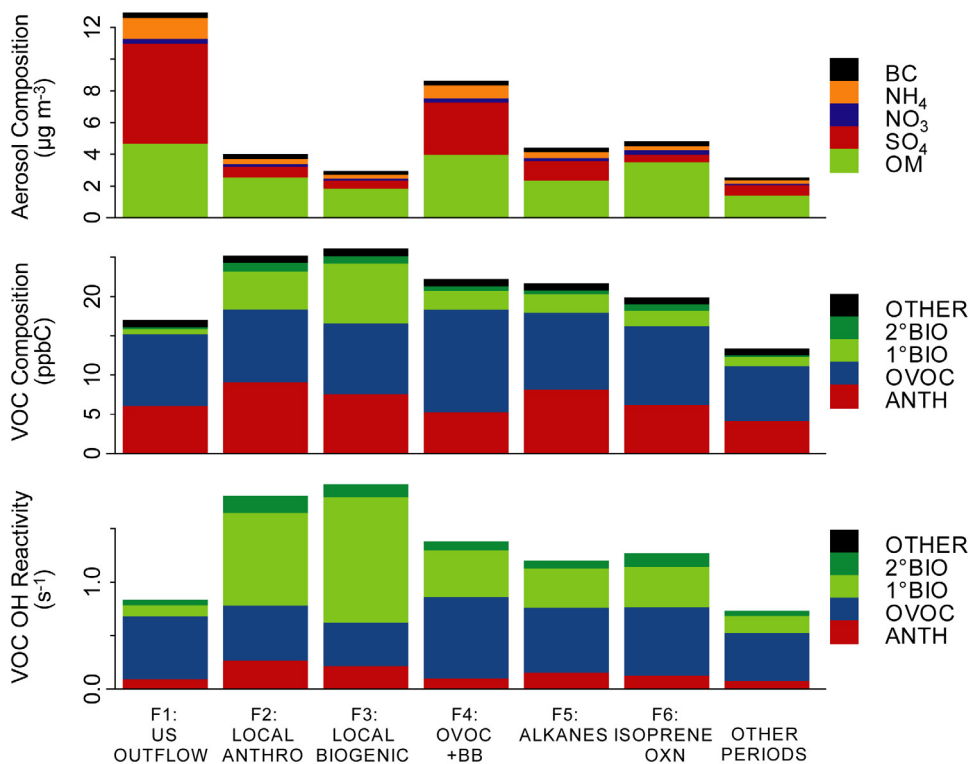


**Figure 8.** Stacked bar plots showing aerosol chemical composition, VOC composition, and VOC OH reactivity during impact periods for each of the six chemical factors and outside of all impact periods. OM, aerosol organic matter; BC, black carbon; ANTH, anthropogenic VOCs; 1°BIO, directly emitted biogenic VOCs; 2°BIO, VOCs photochemically produced from biogenic precursors.

[39] As with the VOC abundance, there is not a significant difference in the average VOC reactivity during U.S. outflow periods ( $0.9 \pm 0.3 \text{ s}^{-1}$ ) compared to other times ( $0.9 \pm 0.6 \text{ s}^{-1}$ ), with a narrower distribution for the former. When the VOC reactivity is broken down by compound class (Figure 8), we see that the biogenic compounds make up a much larger portion of the VOC reactivity than the VOC abundance. This is especially the case during times of local impact, but also during other types of events. Like the

local biogenic (factor 3) events, the local anthropogenic (factor 2) events include a large contribution from biogenic VOC reactivity (Figure 8). Aerosol composition was also similar for factor 2 and 3 events, with a high relative abundance of OM. These two local sources are not perfectly separated using this approach; both are observed with northerly winds from mainland Nova Scotia, most often at night and in the early morning. As a result pollution from

**Table 2.** Aerosol and VOC Composition and Reactivity for Different Event Types<sup>a</sup>

	F1: U.S. Outflow	F2: Local Anthro	F3: Local Biogenic	F4: OVOC+BB	F5: Alkanes	F6: Isoprene Oxn	Other Periods
Aerosol composition, $\mu\text{g m}^{-3}$							
Organic matter	4.70 (2.48)	2.57 (1.72)	1.87 (1.26)	4.00 (2.77)	2.39 (2.31)	3.53 (2.27)	1.41 (1.28)
$\text{SO}_4^{2-}$	6.31 (4.55)	0.67 (0.84)	0.52 (0.47)	3.31 (4.64)	1.21 (1.33)	0.47 (0.40)	0.68 (0.81)
$\text{NO}_3^-$	0.29 (0.30)	0.18 (0.13)	0.12 (0.09)	0.26 (0.21)	0.18 (0.23)	0.28 (0.34)	0.09 (0.11)
$\text{NH}_4^+$	1.33 (0.82)	0.32 (0.26)	0.24 (0.14)	0.83 (0.84)	0.39 (0.32)	0.25 (0.22)	0.22 (0.19)
Black carbon	0.26 (0.15)	0.22 (0.11)	0.15 (0.13)	0.20 (0.14)	0.18 (0.14)	0.23 (0.16)	0.08 (0.07)
VOC composition, ppbC							
Anthropogenic	6.15 (2.13)	9.13 (4.20)	7.63 (4.08)	5.34 (2.07)	8.19 (3.22)	6.26 (2.36)	4.21 (1.81)
Oxygenated	9.10 (2.83)	9.28 (3.24)	9.02 (3.01)	13.02 (3.63)	9.82 (4.92)	10.02 (4.71)	7.00 (3.19)
1° biogenic	0.65 (0.56)	4.83 (4.02)	7.61 (3.42)	2.42 (3.07)	2.35 (3.56)	1.97 (2.19)	1.15 (1.42)
2° biogenic	0.25 (0.18)	1.10 (0.36)	0.93 (0.34)	0.56 (0.45)	0.48 (0.42)	0.84 (0.47)	0.24 (0.25)
Other	0.75 (0.07)	0.75 (0.12)	0.83 (0.12)	0.77 (0.11)	0.76 (0.08)	0.71 (0.08)	0.70 (0.13)
VOC OH reactivity, $\text{s}^{-1}$							
Anthropogenic	0.10 (0.05)	0.27 (0.17)	0.22 (0.14)	0.11 (0.06)	0.16 (0.11)	0.13 (0.08)	0.08 (0.04)
Oxygenated	0.59 (0.29)	0.52 (0.28)	0.41 (0.21)	0.76 (0.33)	0.61 (0.34)	0.64 (0.37)	0.45 (0.26)
1° biogenic	0.10 (0.11)	0.87 (0.63)	1.17 (0.57)	0.44 (0.43)	0.37 (0.54)	0.38 (0.41)	0.16 (0.23)
2° biogenic	0.04 (0.02)	0.15 (0.05)	0.11 (0.04)	0.07 (0.05)	0.06 (0.04)	0.11 (0.06)	0.04 (0.03)

<sup>a</sup>The mean value and standard deviation (in parentheses) are shown.

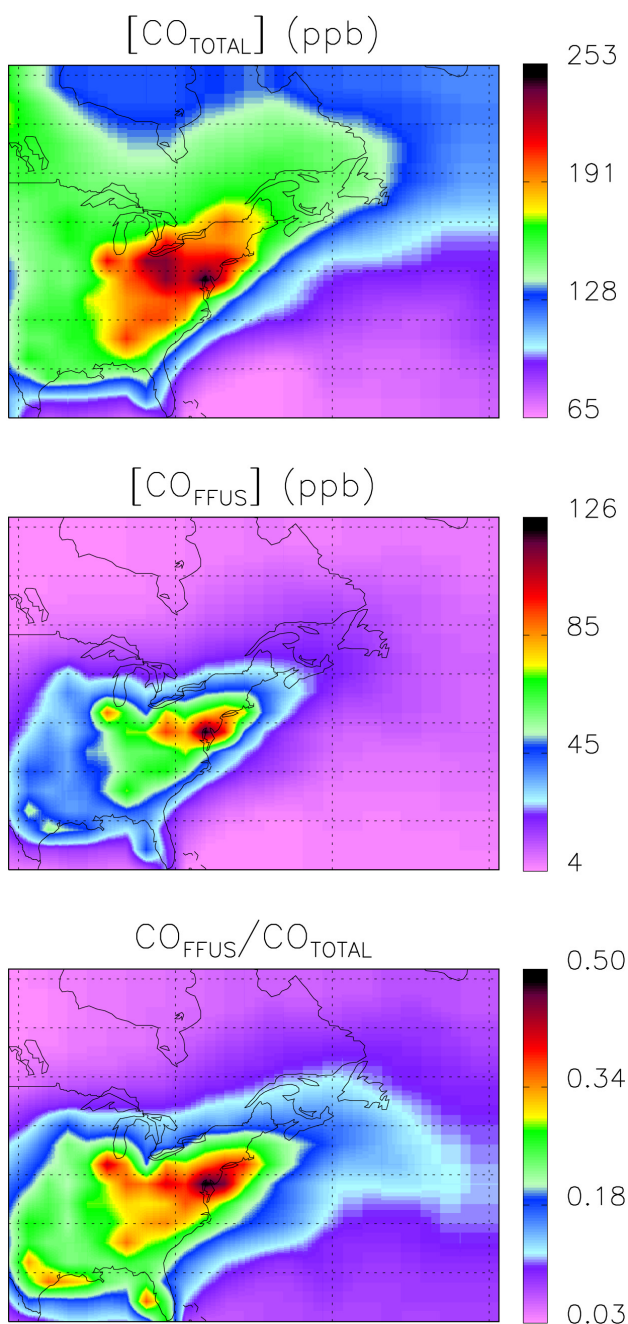


**Figure 9.** Surface level total CO and the amount and fraction of CO from U.S. fossil fuel use, simulated using GEOS-Chem (1 July to 15 August 2004).

Yarmouth is often accompanied by biogenic emissions from the surrounding forests.

[40] Outside of the local influence periods (factors 2 and 3), OVOCs make up the largest fraction of the total OH reactivity. During U.S. outflow events, these compounds account for 71% of the measured reactivity. Highly reactive biogenic compounds such as isoprene and the monoterpenes will have undergone substantial photo-oxidation during transit from the mainland United States, and as a consequence the biogenic gases (primary + secondary) made up a smaller fraction of the total OH reactivity during these times

(17% versus 34%). However, many of the mixed source OVOCs (such as methanol and acetone) have significant biogenic sources as well, and are longer-lived. Consequently, their effect is more widespread. Overall, for the entire data set, the OVOCs and biogenic VOCs make up on average  $\sim 90\%$  of the OH reactivity. This finding is consistent with radiocarbon measurements of formaldehyde at Chebogue Point during NARE-1993 [Tanner *et al.*, 1996], which showed that compound to be 80% modern carbon for all flow regimes. Biogenic emissions thus have a significant impact on the chemistry of air masses at this site, downwind of the polluted northeastern United States.

#### 4. Comparison With Model Results

[41] One great advantage of the factor analysis approach is that it is not subject to errors in modeled emissions, chemistry, or transport. It also offers advantages over using individual tracers for air mass designation, since it provides information on the chemical fingerprint for each source, allows for tracer nonuniqueness (species can load on more than one factor), and does not require prior knowledge of all the important source types. On the other hand, as a correlation-based method, factor analysis informs us only about the sources of variability in the observations, which do not relate directly to actual emission or production rates. Factor analysis is also insensitive to any large but relatively invariant source (for instance, CO production from methane oxidation). In addition, interpreting atmospheric measurements from any stationary platform requires an understanding of the spatial context and representativeness of the site. In this section, we use results from a GEOS-Chem tagged CO simulation to examine these issues. We also assess the degree of consistency between the two methods, and use the model results to place the Chebogue Point findings in the larger context of North American outflow.

[42] Figure 9 shows the spatial distribution of simulated surface level CO (both total and U.S. fossil fuel tagged CO) averaged over the ICARTT-2004 timeframe. From both the discussion above and the model results, we see that even in the marine boundary layer, U.S. pollution outflow repre-

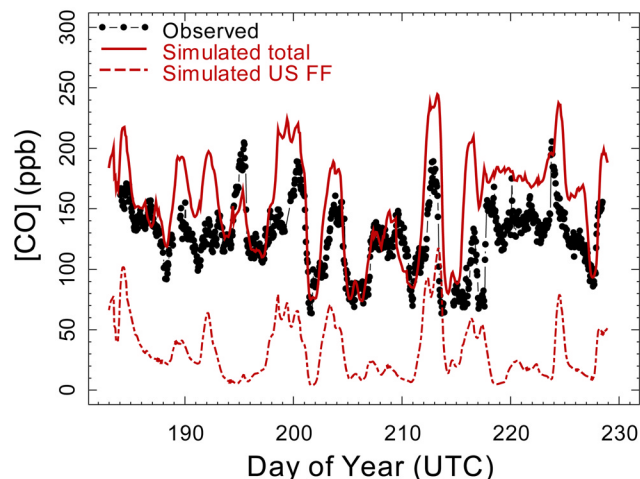


**Figure 10.** CO mixing ratios measured (black) and simulated (red) for Chebogue Point using GEOS-Chem.

**Table 3.** Observed and Simulated CO

	Mean, ppb	0.05–0.95 Quantiles, ppb
Observed CO	126	77–171
Simulated CO		
Total	154	84–218
U.S. fossil fuel	32	7–78
Canada fossil fuel	11	3–22
U.S. + Canada biomass burning	14	2–48
Asia	14	6–22
Europe	3	1–5
Methane and VOC oxidation	70	51–87
Other	10	8–12

sents an important perturbation to atmospheric photochemistry for considerable distances offshore. The tagged tracers include all CO remaining in the atmosphere emitted from a given source, and so the U.S. fossil fuel tracer could contain some influence from recirculated CO (CO emitted from the United States which then circulated around the globe prior to arrival at Chebogue Point). From Figure 9 (middle), however, we see that this is a very minor fraction of the total U.S. pollution CO at Chebogue Point.

[43] Figure 10 displays a timeline of CO mixing ratios measured at Chebogue Point and simulated using the GEOS-Chem CTM. The observed variability is well captured by the model, given the difficulties of simulating atmospheric mixing at coastal sites ( $r^2 = 0.43$ ). The model overestimates observed CO concentrations by an average of 22%, which is similar to the bias found over the northeast United States (19%). This overestimate exists despite a 50% reduction in modeled U.S. on-road CO emissions relative to the EPA NEI99 inventory, as detailed in section 2.2. The fact that the simulated CO increase during U.S. outflow periods (54 ppb) is greater than observed (37 ppb) suggests that the residual model bias relates at least in part to the magnitude and/or spatial distribution of anthropogenic CO emissions from the United States.

[44] We can use the results from the tagged CO simulation to estimate the contributions of different source regions to the observed mixing ratios at Chebogue Point. Direct emissions of CO from North American (U.S. + Canada) fossil fuel and biomass burning make up on average 37% of the total simulated amount at Chebogue Point. Chemical production in the atmosphere from methane and other VOCs averages 45% of the total, with Asian, European, and other sources making up the remainder (Table 3). According to GEOS-Chem, North American fossil fuel

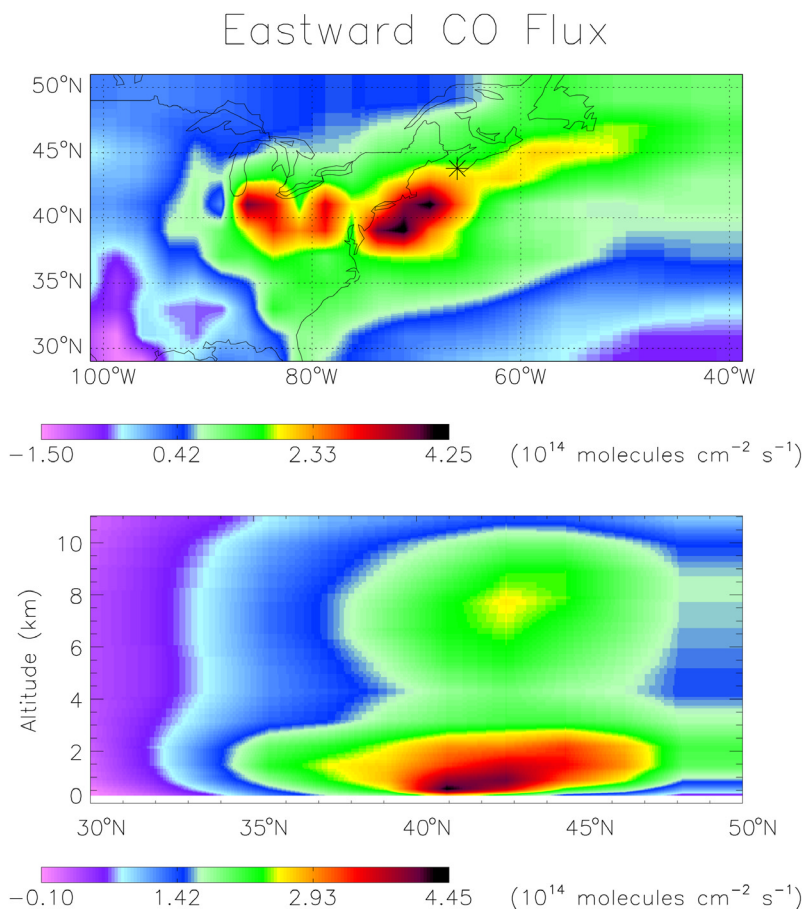


**Figure 11.** Zonal (west-to-east) flux of CO as simulated by GEOS-Chem for July and August 2004 (top) at the surface and (bottom) across a latitude slice at the longitude of Chebogue Point. The location of the site (43.75°N, 66.12°W) is indicated by a star in Figure 11 (top).

emissions account for the majority (68%) of the CO enhancement during U.S. outflow events, and increased chemical production, presumably chiefly from North American precursors, for most of the remainder (26%). The CTM results rely on accurate knowledge of the emission fields: if in fact biases persist in the U.S. CO emission inventory, then the simulated U.S. contribution could be overestimated.

[45] While CO from U.S. pollution sources made up a larger fraction of the total simulated amount during factor 1 impact periods (28%), it was also an important component at other times (19% on average). This does not include CO photochemically produced from North American precursors. The mean contribution of direct emissions from U.S. fossil fuel use to the total modeled CO at the surface is mapped in Figure 9 (bottom). We conclude that the effects of North American pollution on the chemistry of the western North Atlantic boundary layer are ubiquitous and not restricted to particular events.

[46] The GEOS-Chem output also enables us to assess the representativeness of the Chebogue Point data with respect to a broadly defined U.S. outflow. Figure 11 shows the mean simulated zonal (west-to-east) CO flux for July and August 2004 at the surface and across a latitude slice at the longitude of the site. Chebogue Point is clearly well situated to sample surface-layer pollution outflow from the United States. However,  $\sim 70\%$  of the export occurs above 3 km [see also *Li et al.*, 2005], and surface sites such as Chebogue Point cannot be expected to provide an entirely representative picture of that export. On the other hand, they can provide temporal continuity not obtained from aircraft or current satellite instruments. Finally, since the primary motivation for studying pollution transport is the impact on life at the Earth's surface, high-quality surface data are needed to test our understanding of the chemistry of the atmospheric boundary layer and its coupling to the free troposphere.

## 5. Conclusions

[47] We employed extensive chemical measurements of atmospheric composition at Chebogue Point during ICARTT-2004 to examine the chemistry of North American outflow as a function of the dominant source type. By using a chemical factor indicative of U.S. pollution, we show that the criteria pollutants CO, ozone, and submicron aerosol mass are enhanced by 30–300% during U.S. outflow events at this site. Together with oxygenated VOCs, anthropogenic hydrocarbons make up most of the gas phase organic carbon in this region. However, the importance of biogenic species was also evident, both in terms of the photochemical reactivity of the sampled air masses and for the formation of organic aerosol.

[48] The factor analysis-based method used here provides a valuable framework for interpreting chemically and temporally resolved data sets from sites such as Chebogue Point. The approach enabled us to differentiate air masses on the basis of source influence and to define the chemical composition of atmospheric outflow from a given region with a specificity not obtainable with back trajectory or CTM analysis.

[49] Results from a tagged CO simulation using the GEOS-Chem 3D CTM show that Chebogue Point is an appropriate and useful site for sampling the North American plume. However, 70% of the export takes place above 3 km, so that aircraft and satellite observations are also needed to fully characterize North American outflow. According to GEOS-Chem, direct emissions of CO from North American fossil fuel and biomass burning make up on average 37% of the total CO at Chebogue Point, with chemical production in the atmosphere averaging 45%. The model simulation was carried out using a modified version of the EPA NEI99 inventory, with U.S. on-road transport CO emissions reduced by 50%. Our results indicate that biases persist in the inventory which lead to an overestimate of CO at Chebogue Point, particularly during U.S. outflow events. Further work should be done to refine North American emission estimates for CO and other pollutants.

[50] From our analysis of the in situ data and the CTM results, we conclude that the effects of North American air pollution are manifest over a large area of the North Atlantic marine boundary layer.

[51] **Acknowledgments.** This work was supported by the NOAA Office of Global Programs (grant NA16GP2314), the NOAA Aeronomy Laboratory (contracts RA133R-04-SE-0368 and RA133R-05-SE-4459), and the NOAA Climate and Global Change Postdoctoral Fellowship Program (DBM). J.L.J.'s participation in this research was supported by NOAA OGP grant NA05OAR4310025. The authors thank Megan McKay for logistical support and David Parrish and Joost de Gouw for their valuable comments.

## References

- Allan, J. D., J. L. Jimenez, P. I. Williams, M. R. Alfarra, K. N. Bower, J. T. Jayne, H. Coe, and D. R. Worsnop (2003), Quantitative sampling using an Aerodyne aerosol mass spectrometer: 1. Techniques of data interpretation and error analysis, *J. Geophys. Res.*, *108*(D3), 4090, doi:10.1029/2002JD002358.
- Allan, J. D., et al. (2004), A generalized method for the extraction of chemically resolved mass spectra from Aerodyne aerosol mass spectrometer data, *J. Aerosol Sci.*, *35*, 909–922.
- Andreae, M. O., and P. Merlet (2001), Emission of trace gases and aerosols from biomass burning, *Global Biogeochem. Cycles*, *15*(4), 955–966.
- Angevine, W. M., M. P. Buhr, J. S. Holloway, M. Trainer, D. D. Parrish, J. I. MacPherson, G. L. Kok, R. D. Schillawski, and D. H. Bowlby (1996a), Local meteorological features affecting chemical measurements at a North Atlantic coastal site, *J. Geophys. Res.*, *101*(D22), 28,935–28,946.
- Angevine, W. M., M. Trainer, S. A. McKeen, and C. M. Berkowitz (1996b), Mesoscale meteorology of the New England coast, Gulf of Maine, and Nova Scotia: Overview, *J. Geophys. Res.*, *101*(D22), 28,893–28,901.
- Atherton, C. S., S. Sillman, and J. Walton (1996), Three-dimensional global modeling studies of the transport and photochemistry over the North Atlantic Ocean, *J. Geophys. Res.*, *101*(D22), 29,289–29,304.
- Banic, C. M., W. R. Leitch, G. A. Isaac, M. D. Couture, L. I. Kleinman, S. R. Springston, and J. I. MacPherson (1996), Transport of ozone and sulfur to the North Atlantic atmosphere during the North Atlantic Regional Experiment, *J. Geophys. Res.*, *101*(D22), 29,091–29,104.
- Berkowitz, C. M., P. H. Daum, C. W. Spicer, and K. M. Busness (1996), Synoptic patterns associated with the flux of excess ozone to the western North Atlantic, *J. Geophys. Res.*, *101*(D22), 28,923–28,933.
- Buy, I., D. J. Jacob, R. M. Yantosca, J. A. Logan, B. D. Field, A. M. Fiore, Q. B. Li, H. G. Y. Liu, L. J. Mickley, and M. G. Schultz (2001), Global modeling of tropospheric chemistry with assimilated meteorology: Model description and evaluation, *J. Geophys. Res.*, *106*(D19), 23,073–23,095.
- Buhr, M., D. Sueper, M. Trainer, P. Goldan, B. Kuster, F. Fehsenfeld, G. Kok, R. Schillawski, and A. Schanot (1996), Trace gas and aerosol measurements using aircraft data from the North Atlantic Regional Experiment (NARE 1993), *J. Geophys. Res.*, *101*(D22), 29,013–29,027.
- Carter, D. A., K. S. Gage, W. L. Ecklund, W. M. Angevine, P. E. Johnston, A. C. Riddle, J. Wilson, and C. R. Williams (1995), Developments in UHF lower tropospheric wind profiling at NOAA's Aeronomy Laboratory, *Radio Sci.*, *30*(4), 977–1001.

- Daum, P. H., L. I. Kleinman, L. Newman, W. T. Luke, J. Weinstein-Lloyd, C. M. Berkowitz, and K. M. Busness (1996), Chemical and physical properties of plumes of anthropogenic pollutants transported over the North Atlantic during the North Atlantic Regional Experiment, *J. Geophys. Res.*, *101*(D22), 29,029–29,042.
- Day, D. A., P. J. Woodriddle, M. B. Dillon, J. A. Thornton, and R. C. Cohen (2002), A thermal dissociation laser-induced fluorescence instrument for in situ detection of NO<sub>2</sub>, peroxy nitrates, alkyl nitrates, and HNO<sub>3</sub>, *J. Geophys. Res.*, *107*(D6), 4046, doi:10.1029/2001JD000779.
- de Gouw, J. A., et al. (2005), Budget of organic carbon in a polluted atmosphere: Results from the New England Air Quality Study in 2002, *J. Geophys. Res.*, *110*, D16305, doi:10.1029/2004JD005623.
- de Gouw, J. A., et al. (2006), Volatile organic compounds composition of merged and aged forest fire plumes from Alaska and western Canada, *J. Geophys. Res.*, *111*, D10303, doi:10.1029/2005JD006175.
- Delene, D. J., and J. A. Ogren (2002), Variability of aerosol optical properties at four North American surface monitoring sites, *J. Atmos. Sci.*, *59*(6), 1135–1150.
- Draxler, R. R. (1996), Boundary layer isentropic and kinematic trajectories during the August 1993 North Atlantic Regional Experiment Intensive, *J. Geophys. Res.*, *101*(D22), 29,255–29,268.
- Fast, J. D., and C. M. Berkowitz (1996), A modeling study of boundary layer processes associated with ozone layers observed during the 1993 North Atlantic Regional Experiment, *J. Geophys. Res.*, *101*(D22), 28,683–28,699.
- Fehsenfeld, F. C., P. Daum, W. R. Leitch, M. Trainer, D. D. Parrish, and G. Hubler (1996), Transport and processing of O<sub>3</sub> and O<sub>3</sub> precursors over the North Atlantic: An overview of the 1993 North Atlantic Regional Experiment (NARE) summer intensive, *J. Geophys. Res.*, *101*(D22), 28,877–28,891.
- Goldan, P. D., M. Trainer, W. C. Kuster, D. D. Parrish, J. Carpenter, J. M. Roberts, J. E. Yee, and F. C. Fehsenfeld (1995), Measurements of hydrocarbons, oxygenated hydrocarbons, carbon monoxide, and nitrogen oxides in an urban Basin in Colorado: Implications for emission inventories, *J. Geophys. Res.*, *100*(D11), 22,771–22,783.
- Goldstein, A. H., S. M. Fan, M. L. Goulden, J. W. Munger, and S. C. Wofsy (1996), Emissions of ethene, propene, and 1-butene by a midlatitude forest, *J. Geophys. Res.*, *101*(D4), 9149–9157.
- Goode, J. G., R. J. Yokelson, D. E. Ward, R. A. Susott, R. E. Babbitt, M. A. Davies, and W. M. Hao (2000), Measurements of excess O<sub>3</sub>, CO<sub>2</sub>, CO, CH<sub>4</sub>, C<sub>2</sub>H<sub>4</sub>, C<sub>2</sub>H<sub>2</sub>, HCN, NO, NH<sub>3</sub>, HCOOH, CH<sub>3</sub>COOH, HCHO, and CH<sub>3</sub>OH in 1997 Alaskan biomass burning plumes by airborne fourier transform infrared spectroscopy (AFTIR), *J. Geophys. Res.*, *105*(D17), 22,147–22,166.
- Grosjean, D., E. Grosjean, and A. W. Gertler (2001), On-road emissions of carbonyls from light-duty and heavy-duty vehicles, *Environ. Sci. Technol.*, *35*(1), 45–53.
- Heald, C. L., D. J. Jacob, R. J. Park, L. M. Russell, B. J. Huebert, J. H. Seinfeld, H. Liao, and R. J. Weber (2005), A large organic aerosol source in the free troposphere missing from current models, *Geophys. Res. Lett.*, *32*, L18809, doi:10.1029/2005GL023831.
- Holzinger, R., C. Warneke, A. Hansel, A. Jordan, W. Lindinger, D. H. Scharffe, G. Schade, and P. J. Crutzen (1999), Biomass burning as a source of formaldehyde, acetaldehyde, methanol, acetone, acetonitrile, and hydrogen cyanide, *Geophys. Res. Lett.*, *26*(8), 1161–1164.
- Holzinger, R., J. Williams, G. Salisbury, T. Klupfel, M. de Reus, M. Traub, P. J. Crutzen, and J. Lelieveld (2005), Oxygenated compounds in aged biomass burning plumes over the Eastern Mediterranean: Evidence for strong secondary production of methanol and acetone, *Atmos. Chem. Phys.*, *5*, 39–46.
- Horowitz, L. W., J. Y. Liang, G. M. Gardner, and D. J. Jacob (1998), Export of reactive nitrogen from North America during summertime: Sensitivity to hydrocarbon chemistry, *J. Geophys. Res.*, *103*(D11), 13,451–13,476.
- Jacob, D. J., B. D. Field, E. M. Jin, I. Bey, Q. B. Li, J. A. Logan, R. M. Yantosca, and H. B. Singh (2002), Atmospheric budget of acetone, *J. Geophys. Res.*, *107*(D10), 4100, doi:10.1029/2001JD000694.
- Jacob, D. J., B. D. Field, Q. B. Li, D. R. Blake, J. de Gouw, C. Warneke, A. Hansel, A. Wisthaler, H. B. Singh, and A. Guenther (2005), Global budget of methanol: Constraints from atmospheric observations, *J. Geophys. Res.*, *110*, D08303, doi:10.1029/2004JD005172.
- Jayne, J. T., D. C. Leard, X. F. Zhang, P. Davidovits, K. A. Smith, C. E. Kolb, and D. R. Worsnop (2000), Development of an aerosol mass spectrometer for size and composition analysis of submicron particles, *Aerosol Sci. Technol.*, *33*(1–2), 49–70.
- Jimenez, J. L., et al. (2003), Ambient aerosol sampling using the Aerodyne Aerosol Mass Spectrometer, *J. Geophys. Res.*, *108*(D7), 8425, doi:10.1029/2001JD001213.
- Jost, C., J. Trentmann, D. Sprung, M. O. Andreae, J. B. McQuaid, and H. Barjat (2003), Trace gas chemistry in a young biomass burning plume over Namibia: Observations and model simulations, *J. Geophys. Res.*, *108*(D13), 8482, doi:10.1029/2002JD002431.
- Karl, T., A. Guenther, C. Spirig, A. Hansel, and R. Fall (2003), Seasonal variation of biogenic VOC emissions above a mixed hardwood forest in northern Michigan, *Geophys. Res. Lett.*, *30*(23), 2186, doi:10.1029/2003GL018432.
- Kasibhatla, P., H. Levy, A. Klonecki, and W. L. Chameides (1996), Three-dimensional view of the large-scale tropospheric ozone distribution over the North Atlantic Ocean during summer, *J. Geophys. Res.*, *101*(D22), 29,305–29,316.
- Kellerhals, M., et al. (2003), Temporal and spatial variability of total gaseous mercury in Canada: Results from the Canadian Atmospheric Mercury Measurement Network (CAMNet), *Atmos. Environ.*, *37*(7), 1003–1011.
- Kim, E., S. G. Brown, H. R. Hafner, and P. K. Hopke (2005), Characterization of non-methane volatile organic compounds sources in Houston during 2001 using positive matrix factorization, *Atmos. Environ.*, *39*(32), 5934–5946.
- Kleinman, L. I., P. H. Daum, Y. N. Lee, S. R. Springston, L. Newman, W. R. Leitch, C. M. Banic, G. A. Isaac, and J. I. MacPherson (1996), Measurement of O<sub>3</sub> and related compounds over southern Nova Scotia: 1. Vertical distributions, *J. Geophys. Res.*, *101*(D22), 29,043–29,060.
- Knapp, K. G., B. B. Balsley, M. L. Jensen, H. P. Hanson, and J. W. Birks (1998), Observation of the transport of polluted air masses from the northeastern United States to Cape Sable Island, Nova Scotia, Canada, during the 1993 NARE summer intensive, *J. Geophys. Res.*, *103*(D11), 13,399–13,411.
- Lamanna, M. S., and A. H. Goldstein (1999), In situ measurements of C<sub>2</sub>–C<sub>10</sub> volatile organic compounds above a Sierra Nevada ponderosa pine plantation, *J. Geophys. Res.*, *104*(D17), 21,247–21,262.
- Lelieveld, J., J. van Aardenne, H. Fischer, M. de Reus, J. Williams, and P. Winkler (2004), Increasing ozone over the Atlantic Ocean, *Science*, *304*(5676), 1483–1487.
- Li, Q. B., D. J. Jacob, R. M. Yantosca, C. L. Heald, H. B. Singh, M. Koike, Y. J. Zhao, G. W. Sachse, and D. G. Streets (2003), A global three-dimensional model analysis of the atmospheric budgets of HCN and CH<sub>3</sub>CN: Constraints from aircraft and ground measurements, *J. Geophys. Res.*, *108*(D21), 8827, doi:10.1029/2002JD003075.
- Li, Q. B., D. J. Jacob, J. W. Munger, R. M. Yantosca, and D. D. Parrish (2004), Export of NO<sub>y</sub> from the North American boundary layer: Reconciling aircraft observations and global model budgets, *J. Geophys. Res.*, *109*, D02313, doi:10.1029/2003JD004086.
- Li, Q. B., D. J. Jacob, R. Park, Y. X. Wang, C. L. Heald, R. Hudman, R. M. Yantosca, R. V. Martin, and M. Evans (2005), North American pollution outflow and the trapping of convectively lifted pollution by upper-level anticyclone, *J. Geophys. Res.*, *110*, D10301, doi:10.1029/2004JD005039.
- Liang, J. Y., L. W. Horowitz, D. J. Jacob, Y. H. Wang, A. M. Fiore, J. A. Logan, G. M. Gardner, and J. W. Munger (1998), Seasonal budgets of reactive nitrogen species and ozone over the United States, and export fluxes to the global atmosphere, *J. Geophys. Res.*, *103*(D11), 13,435–13,450.
- Lindinger, W., A. Hansel, and A. Jordan (1998), On-line monitoring of volatile organic compounds at pptv levels by means of proton-transfer-reaction mass spectrometry (PTR-MS)—Medical applications, food control and environmental research, *Int. J. Mass Spectrom.*, *173*(3), 191–241.
- Lobert, J. M., D. H. Scharffe, W. M. Hao, and P. J. Crutzen (1990), Importance of biomass burning in the atmospheric budgets of nitrogen-containing gases, *Nature*, *346*(6284), 552–554.
- Maria, S. F., and L. M. Russell (2005), Organic and inorganic aerosol below-cloud scavenging by suburban New Jersey precipitation, *Environ. Sci. Technol.*, *39*(13), 4793–4800.
- Martin, R. V., et al. (2002), Interpretation of TOMS observations of tropical tropospheric ozone with a global model and in situ observations, *J. Geophys. Res.*, *107*(D18), 4351, doi:10.1029/2001JD001480.
- Merrill, J. T., and J. L. Moody (1996), Synoptic meteorology and transport during the North Atlantic Regional Experiment (NARE) intensive: Overview, *J. Geophys. Res.*, *101*(D22), 28,903–28,921.
- Millet, D. B., et al. (2004), Volatile organic compound measurements at Trinidad Head, California during ITCT 2K2: Analysis of sources, atmospheric composition and aerosol residence times, *J. Geophys. Res.*, *109*, D23S16, doi:10.1029/2003JD004026.
- Millet, D. B., N. M. Donahue, S. N. Pandis, A. Polidori, C. O. Stanier, B. J. Turpin, and A. H. Goldstein (2005), Atmospheric volatile organic compound measurements during the Pittsburgh Air Quality Study: Results, interpretation and quantification of primary and secondary contributions, *J. Geophys. Res.*, *110*, D07S07, doi:10.1029/2004JD004601.
- Moody, J. L., J. C. Davenport, J. T. Merrill, S. J. Oltmans, D. D. Parrish, J. S. Holloway, H. Levy, G. L. Forbes, M. Trainer, and M. Buhr (1996), Meteorological mechanisms for transporting O<sub>3</sub> over the western North

- Atlantic ocean: A case study for August 24–29, 1993, *J. Geophys. Res.*, *101*(D22), 29,213–29,227.
- Oltmans, S. J., et al. (1996), Summer and spring ozone profiles over the North Atlantic from ozonesonde measurements, *J. Geophys. Res.*, *101*(D22), 29,179–29,200.
- Park, R. J., D. J. Jacob, B. D. Field, R. M. Yantosca, and M. Chin (2004), Natural and transboundary pollution influences on sulfate-nitrate-ammonium aerosols in the United States: Implications for policy, *J. Geophys. Res.*, *109*, D15204, doi:10.1029/2003JD004473.
- Parrish, D. D. (2006), Critical evaluation of US on-road vehicle emission inventories, *Atmos. Environ.*, *40*, 2288–2300.
- Parrish, D. D., J. S. Holloway, M. Trainer, P. C. Murphy, G. L. Forbes, and F. C. Fehsenfeld (1993), Export of North American ozone pollution to the North Atlantic Ocean, *Science*, *259*(5100), 1436–1439.
- Parrish, D. D., M. Trainer, J. S. Holloway, J. E. Yee, M. S. Warshawsky, F. C. Fehsenfeld, G. L. Forbes, and J. L. Moody (1998), Relationships between ozone and carbon monoxide at surface sites in the North Atlantic region, *J. Geophys. Res.*, *103*(D11), 13,357–13,376.
- Pfister, G., P. G. Hess, L. K. Emmons, J. F. Lamarque, C. Wiedinmyer, D. P. Edwards, G. Petron, J. C. Gille, and G. W. Sachse (2005), Quantifying CO emissions from the 2004 Alaskan wildfires using MOPITT CO data, *Geophys. Res. Lett.*, *32*, L11809, doi:10.1029/2005GL022995.
- Quinn, P. K., et al. (2000), Surface submicron aerosol chemical composition: What fraction is not sulfate?, *J. Geophys. Res.*, *105*(D5), 6785–6805.
- Roberts, J. M., et al. (1996), Episodic removal of NO<sub>y</sub> species from the marine boundary layer over the North Atlantic, *J. Geophys. Res.*, *101*(D22), 28,947–28,960.
- Roberts, J. M., S. B. Bertman, T. Jobson, H. Niki, and R. Tanner (1998), Measurement of total nonmethane organic carbon (C<sub>y</sub>): Development and application at Chebogue Point, Nova Scotia, during the 1993 North Atlantic Regional Experiment campaign, *J. Geophys. Res.*, *103*(D11), 13,581–13,592.
- Roberts, J. M., F. Flocke, C. A. Stroud, D. Hereid, E. Williams, F. Fehsenfeld, W. Brune, M. Martinez, and H. Harder (2002), Ground-based measurements of peroxy-carboxylic nitric anhydrides (PANs) during the 1999 Southern Oxidants Study Nashville Intensive, *J. Geophys. Res.*, *107*(D21), 4554, doi:10.1029/2001JD000947.
- Schade, G. W., and A. H. Goldstein (2001), Fluxes of oxygenated volatile organic compounds from a ponderosa pine plantation, *J. Geophys. Res.*, *106*(D3), 3111–3123.
- Sheridan, P. J., D. J. Delene, and J. A. Ogren (2001), Four years of continuous surface aerosol measurements from the Department of Energy's Atmospheric Radiation Measurement Program Southern Great Plains Cloud and Radiation Testbed site, *J. Geophys. Res.*, *106*(D18), 20,735–20,747.
- Stohl, A., and D. J. Thomson (1999), A density correction for Lagrangian particle dispersion models, *Boundary Layer Meteorol.*, *90*(1), 155–167.
- Stohl, A., and T. Trickl (1999), A textbook example of long-range transport: Simultaneous observation of ozone maxima of stratospheric and North American origin in the free troposphere over Europe, *J. Geophys. Res.*, *104*(D23), 30,445–30,462.
- Stohl, A., M. Hittenberger, and G. Wotawa (1998), Validation of the Lagrangian particle dispersion model FLEXPART against large-scale tracer experiment data, *Atmos. Environ.*, *32*(24), 4245–4264.
- Tanner, R. L., B. Zielinska, E. Uberna, G. Harshfield, and A. P. McNichol (1996), Concentrations of carbonyl compounds and the carbon isotopy of formaldehyde at a coastal site in Nova Scotia during the NARE summer intensive, *J. Geophys. Res.*, *101*(D22), 28,961–28,970.
- Trentmann, J., R. J. Yokelson, P. V. Hobbs, T. Winterrath, T. J. Christian, M. O. Andreae, and S. A. Mason (2005), An analysis of the chemical processes in the smoke plume from a savanna fire, *J. Geophys. Res.*, *110*, D12301, doi:10.1029/2004JD005628.
- VanCuren, R. A., S. S. Cliff, K. D. Perry, and M. Jimenez-Cruz (2005), Asian continental aerosol persistence above the marine boundary layer over the eastern North Pacific: Continuous aerosol measurements from Intercontinental Transport and Chemical Transformation 2002 (ITCT K22), *J. Geophys. Res.*, *110*, D09S90, doi:10.1029/2004JD004973.
- Wang, T., et al. (1996), Ground-based measurements of NO<sub>x</sub> and total reactive oxidized nitrogen (NO<sub>y</sub>) at Sable Island, Nova Scotia, during the NARE 1993 summer intensive, *J. Geophys. Res.*, *101*(D22), 28,991–29,004.
- Wang, Y. H., et al. (2003), Intercontinental transport of pollution manifested in the variability and seasonal trend of springtime O<sub>3</sub> at northern middle and high latitudes, *J. Geophys. Res.*, *108*(D21), 4683, doi:10.1029/2003JD003592.
- Williams, B. J., A. H. Goldstein, N. M. Kreisberg, and S. V. Hering (2006), An in-situ instrument for speciated organic composition of atmospheric aerosols: Thermal Desorption Aerosol GC/MS-FID (TAG), *Aerosol Sci. Technol.*, *40*(8), 627–638.
- Williams, J., et al. (2000), A method for the airborne measurement of PAN, PPN, and MPAN, *J. Geophys. Res.*, *105*(D23), 28,943–28,960.
- Xiao, Y. P., D. J. Jacob, J. S. Wang, J. A. Logan, P. I. Palmer, P. Suntharalingam, R. M. Yantosca, G. W. Sachse, D. R. Blake, and D. G. Streets (2004), Constraints on Asian and European sources of methane from CH<sub>4</sub>-C<sub>2</sub>H<sub>6</sub>-CO correlations in Asian outflow, *J. Geophys. Res.*, *109*, D15S16, doi:10.1029/2003JD004475.
- Yokelson, R. J., D. W. T. Griffith, and D. E. Ward (1996), Open-path Fourier transform infrared studies of large-scale laboratory biomass fires, *J. Geophys. Res.*, *101*(D15), 21,067–21,080.
- Yokelson, R. J., I. T. Bertsch, T. J. Christian, P. V. Hobbs, D. E. Ward, and W. M. Hao (2003), Trace gas measurements in nascent, aged, and cloud-processed smoke from African savanna fires by airborne Fourier transform infrared spectroscopy (AFTIR), *J. Geophys. Res.*, *108*(D13), 4683, doi:10.1029/2003JD003592.

J. D. Allan, School of Earth, Atmospheric and Environmental Science, University of Manchester, Manchester M13 9PL, UK.

I. T. Bertsch, Hoefler Consulting Group, Inc., Anchorage, AK 99503, USA.

A. H. Goldstein and B. J. Williams, Division of Ecosystem Sciences, University of California, Berkeley, CA 94720, USA.

R. Holzinger, Institute for Marine and Atmospheric Research, Utrecht University, NL-3508 TA Utrecht, Netherlands.

R. C. Hudman, Division of Engineering and Applied Sciences, Harvard University, Cambridge, MA 02138, USA.

J. L. Jimenez, Department of Chemistry, University of Colorado, Boulder, CO 80309, USA.

D. B. Millet, Department of Earth and Planetary Sciences, Harvard University, Cambridge, MA 02138, USA. (dbm@io.harvard.edu)

J. M. Roberts and A. B. White, NOAA Earth System Research Laboratory, Boulder, CO 80305, USA.

A. Stohl, Norwegian Institute for Air Research, N-2027 Kjeller, Norway.

D. R. Worsnop, Aerodyne Research Incorporated, Billerica, MA 01821, USA.